Journal of Chemical Physics **128** (2008) 154506 (*7 pages*)

# Fluctuation theorem and mesoscopic chemical clocks

David Andrieux and Pierre Gaspard
*Center for Nonlinear Phenomena and Complex Systems,*
*Université Libre de Bruxelles, Code Postal 231, Campus Plaine, B-1050 Brussels, Belgium*

The fluctuation theorems for dissipation and the currents are applied to the stochastic version of the reversible Brusselator model of nonequilibrium oscillating reactions. It is verified that the symmetry of these theorems holds far from equilibrium in the regimes of noisy oscillations. Moreover, the fluctuation theorem for the currents is also verified for a truncated Brusselator model.

PACS numbers: 82.20.Uv; 05.70.Ln; 02.50.Ey

## I. INTRODUCTION

The so-called fluctuation theorems suggest that general relationships might hold for fluctuations in nonequilibrium systems [1–16]. In such systems, these relationships establish a symmetry between the forward and reversed fluctuations of dissipation or currents, showing that the ratio of their probability distributions is related to the De Donder affinities, i.e., the thermodynamic forces driving the system out of equilibrium [17]. The fluctuation theorems appear to play an important role in nonequilibrium statistical thermodynamics because they allow us to obtain results generalizing Onsager's reciprocity relations to the nonlinear response coefficients [13, 16]. Albeit early work has envisaged such relationships in mechanical systems, they have recently been extended to reacting systems described by stochastic processes [9, 12–14]. In this context, we may wonder how far from equilibrium the fluctuation theorems might hold. Such a theorem has already been shown to hold in bistable nonequilibrium reactions as in the Schlögl model [12].

In the present paper, our purpose is to show that the fluctuation theorems also apply to mesoscopic chemical clocks [18–21]. Such clocks exist not only at the macroscopic scale in the Belousov-Zhabotinsky reaction [22, 23], the bromate-iodide reaction [24], the chlorite-based reactions [25], biochemical reactions [26, 27], and heterogeneous catalysis [28, 29], but also at the nanoscale under field emission microscopy conditions [30–32]. At the nanoscale, the reactions are affected by molecular fluctuations due to the limited numbers of molecules in these systems. Accordingly, reactions at the nanoscale are described as birth-and-death stochastic processes ruled by a master equation [19, 33–36]. The vehicle of our demonstration is the Brusselator model of chemical oscillations [37, 38]. Since the fluctuation theorem compares forward with reversed fluctuations, it is essential to include the reversed reactions in the chemical network of the Brusselator.

In this model, we first consider the fluctuation theorem for dissipation [5, 12]. This theorem concerns a fluctuating quantity which measures the breaking of detailed balance that arises if a system is driven out of equilibrium. This so-called action functional fluctuates around a mean drift which grows linearly in time at a rate precisely given by the thermodynamic entropy production [5, 12]. At equilibrium, the entropy production vanishes and the forward and reversed fluctuations are in balance for each reaction. Although this detailed balance is broken out of equilibrium, the remarkable result is that a symmetry coming from the microreversibility still holds far from equilibrium in oscillating regimes.

We also consider the fluctuation theorem for the currents or fluxes of matter from reactants to products [13, 15]. Since the oscillations emerge far from equilibrium, the system is crossed by net currents or fluxes from high to low free enthalpy species. The difference of free enthalpies between reactants and products defines the De Donder affinity driving the reaction [17]. The fluctuations of the currents or fluxes also obey a symmetry relation similar to the fluctuation theorem for dissipation, as shown elsewhere [13, 15]. We here verify that this symmetry is indeed satisfied in the far-from-equilibrium regimes of oscillations.

The paper is organized as follows. In Sec. II, we introduce the stochastic model of the reversible Brusselator. The fluctuation theorem for dissipation is verified in Sec. III and the one for the currents in Sec. IV. In Sec. V, the fluctuation theorem for the currents is verified in a truncated model keeping two out of the three reactions of the Brusselator. Conclusions are drawn in Sec. VI.

## II. THE BRUSSELATOR MODEL OF OSCILLATIONS

The Brusselator is a reaction network which has been proposed as a model of nonequilibrium oscillations [37, 38]. This model shows that the oscillations may arise in autocatalytic reaction networks with at least two intermediate species. The autocatalysis is at the origin of the nonlinearity responsible for the oscillations. The Brusselator may be considered in its irreversible or reversible versions, which both sustain limit cycle oscillations. For our purposes, we consider the reversible Brusselator which include both the forward and reversed reactions [38]:

$$\mathrm{A} \underset{k_{-1}}{\overset{k_{+1}}{\rightleftharpoons}} \mathrm{X} \tag{1}$$

$$\mathrm{B} + \mathrm{X} \underset{k_{-2}}{\overset{k_{+2}}{\rightleftharpoons}} \mathrm{Y} + \mathrm{C} \tag{2}$$

$$2\mathrm{X} + \mathrm{Y} \underset{k_{-3}}{\overset{k_{+3}}{\rightleftharpoons}} 3\mathrm{X} \tag{3}$$

The species A, B, and C are supposed to enter the system with the constant concentrations [A], [B], and [C]. This can be achieved either if these species arrive from separate external reservoirs or if their concentration is so high with respect to the concentrations of the intermediate species X and Y and they can be assumed to remain constant in time. The quantities $k_\rho$ are the reaction constants, which are independent of the concentrations. The reactions are supposed to take place under isothermal conditions. We notice that the trimolecular reaction network (1)-(3) can be conceived as the reduction of a larger bimolecular reaction network [39].

In the following, we present the description of the reversible Brusselator, first, in the framework of macroscopic kinetics and, secondly, at the mesoscopic level, as a birth-and-death stochastic process.

### A. The macroscopic level

At the macroscopic level, the time evolution of the system is monitored in terms of the concentrations of the intermediate species, $x = [\mathrm{X}]$ and $y = [\mathrm{Y}]$. The equations for these concentrations are established by the mass action law of kinetics as

$$\frac{dx}{dt} = k_{+1}\,[\mathrm{A}] - k_{-1}x + k_{-2}\,[\mathrm{C}]\,y - k_{+2}\,[\mathrm{B}]\,x + k_{+3}x^2y - k_{-3}x^3 \tag{4}$$

$$\frac{dy}{dt} = k_{+2}\,[\mathrm{B}]\,x - k_{-2}\,[\mathrm{C}]\,y + k_{-3}x^3 - k_{+3}x^2y \tag{5}$$

The unique steady state of the system is given by

$$x_\mathrm{s} = \frac{k_{+1}}{k_{-1}}\,[\mathrm{A}] \tag{6}$$

$$y_\mathrm{s} = x_\mathrm{s}\,\frac{k_{+2}\,[\mathrm{B}] + k_{-3}x_\mathrm{s}^2}{k_{-2}\,[\mathrm{C}] + k_{+3}x_\mathrm{s}^2} \tag{7}$$

The linear stability analysis indicates that this steady state is a stable node in the vicinity of equilibrium to become a stable focus further away for equilibrium. A stable node is a steady state with two negative real stability eigenvalues, and a stable focus has two complex conjugate stability eigenvalues with a negative real part [40]. As the nonequilibrium constraint is increased, the steady state can loose its stability and undergo a Hopf bifurcation leading to a limit cycle. A limit cycle is a solution of the set of ordinary differential equations (4)-(5) which is periodic in time and which represents the oscillations of the macroscopic concentrations [40]. In dissipative systems such as the Brusselator, the limit cycle is attracting so that trajectories from nearby initial conditions converge toward the limit cycle, which is robust in this sense. The limit cycle is a closed orbit encircling the steady state (6)-(7) in the phase space of the Brusselator composed of the non-negative quadrant of the two-dimensional plane $(x, y)$.

The equilibrium states are identified thank to the conditions of detailed balance that each forward reaction is balanced by the corresponding reversed reaction. Accordingly, the equilibrium concentrations are given by

$$x_\mathrm{eq} = \frac{k_{+1}}{k_{-1}}\,[\mathrm{A}] \tag{8}$$

$$y_\mathrm{eq} = x_\mathrm{eq}\,\frac{k_{+2}\,[\mathrm{B}]}{k_{-2}\,[\mathrm{C}]} = x_\mathrm{eq}\,\frac{k_{-3}}{k_{+3}} \tag{9}$$

leading to the following equilibrium condition:

$$k_{+3}k_{+2}\,[\mathrm{B}] = k_{-3}k_{-2}\,[\mathrm{C}] \tag{10}$$

between the concentrations of the species B and C. Therefore, there is only one possible nonequilibrium constraint in this model and one associated flux corresponding to the overall reaction $\mathrm{B} \rightarrow \mathrm{C}$.

### B. The mesoscopic level

At the mesoscopic level, the molecular fluctuations are important and the reactive events of the chemical network (1)-(3) randomly happen in time. Accordingly, the reactions are described as a birth-and-death stochastic process for the numbers, $X(t)$ and $Y(t)$, of molecules of the intermediate species. At each reactive event, these numbers undergo a jump by integer values corresponding to the stoichiometric coefficients of the reaction. This stochastic process is ruled by a Markovian master equation for the probability $P(X, Y; t)$ that the system contains the numbers $X$ and $Y$ of molecules at time $t$ [12, 13, 19, 33–36]. For the reversible Brusselator, the transitions rates of the master equation are given by

$$W_{+1}(X, Y|X+1, Y) = k_{+1}\ \ [\mathrm{A}]\,\Omega \tag{11}$$

$$W_{-1}(X, Y|X-1, Y) = k_{-1}X \tag{12}$$

$$W_{+2}(X, Y|X-1, Y+1) = k_{+2}\,[\mathrm{B}]\,X \tag{13}$$

$$W_{-2}(X, Y|X+1, Y-1) = k_{-2}\,[\mathrm{C}]\,Y \tag{14}$$

$$W_{+3}(X, Y|X+1, Y-1) = k_{+3}\frac{X(X-1)Y}{\Omega^2} \tag{15}$$

$$W_{-3}(X, Y|X-1, Y+1) = k_{-3}\frac{X(X-1)(X-2)}{\Omega^2} \tag{16}$$

where $\Omega$ is a extensivity parameter characterizing the volume of the system. These transition rates are compatible with the mass action law of kinetics [19, 33–36]. The concentrations of the intermediate species can be obtained by averaging the molecular numbers with the probability distribution and dividing by the extensivity parameter. In the macroscopic limit where the fluctuations become negligible, it has been shown that the macroscopic kinetic equations (4)-(5) are recovered.

The birth-and-death stochastic process can be simulated numerically by an algorithm proposed by Gillespie [41, 42]. The waiting times between the random jumps have exponential probability distributions. At each step of the stochastic process, pseudo-random generators determine the jump in $X$ and $Y$ as well as the corresponding waiting time according to probabilities given by the transition rates (11)-(16). As a result, the Gillespie algorithm will generate a random path:

$$(X_0, Y_0) \xrightarrow{\rho_1} (X_1, Y_1) \xrightarrow{\rho_2} (X_2, Y_2) \xrightarrow{\rho_3} \cdots \xrightarrow{\rho_n} (X_n, Y_n) \xrightarrow{\rho_{n+1}} \cdots \tag{17}$$

with jumps due to the reactive events $\rho_1, \rho_2, ..., \rho_n, ...$ occurring at the successive times $0 < t_1 < t_2 < \cdots < t_n < \cdots$.

The master equation of the reversible Brusselator admits a stationary distribution, such that $(d/dt)P_{\mathrm{st}}(X, Y) = 0$. We notice that the transition rates (11)-(16) depend on the constant concentrations of the reactants. It is through these concentrations that the system can be driven out of equilibrium. Indeed, it is only if the concentrations take their equilibrium values (10) that the statistical distribution $P_{\mathrm{eq}}(X, Y)$ corresponding to the state of thermodynamic equilibrium is found. Otherwise, the master equation will describe a genuine nonequilibrium state. Beside the stationary solution, the master equation admits time-dependent solutions starting from some nonequilibrium initial probability distribution and this under both equilibrium and nonequilibrium conditions. However, the master equation is known to obey a $H$-theorem so that these time-dependent solutions typically converge toward the corresponding stationary solution [12, 13, 35].

The question therefore arises how to identify the nonequilibrium oscillations in the stochastic framework. Even in the regimes where the macroscopic kinetic equations (4)-(5) admit a time-periodic solution, the master equation continues to admit a stationary solution $P_{\mathrm{st}}(X, Y)$. The fact is that the limit cycle manifests itself in the stationary distribution by the crater-like shape of this latter when plotted in the plane $(X, Y)$. Indeed, this particular shape is induced because the probability is the highest along the closed orbit of the limit cycle and is spread in its vicinity due to the fluctuations. It is only in the macroscopic limit $\Omega \rightarrow \infty$ that the fluctuations become negligible so that the probability distribution is entirely supported by the closed orbit.

Another characterization goes by considering time-dependent properties such as the autocorrelation functions of the concentrations [43]

$$C_{XX}(t) = \frac{\langle X(t)X(0)\rangle}{\langle X\rangle^2} - 1 \sim \mathrm{e}^{-\gamma t}\cos(\omega t + \phi) \tag{18}$$

which typically present damped oscillations. The correlation time $\gamma^{-1}$ can be calculated by the Hamilton-Jacobi method in the weak noise limit [43]. It turns out that the correlation time is proportional to the extensivity parameter $\gamma^{-1} \sim \Omega$. Hence, the correlation time becomes infinite in the macroscopic limit, in which case we recover a strictly periodic behavior. Otherwise the oscillations are affected by the molecular fluctuations and are irregular.

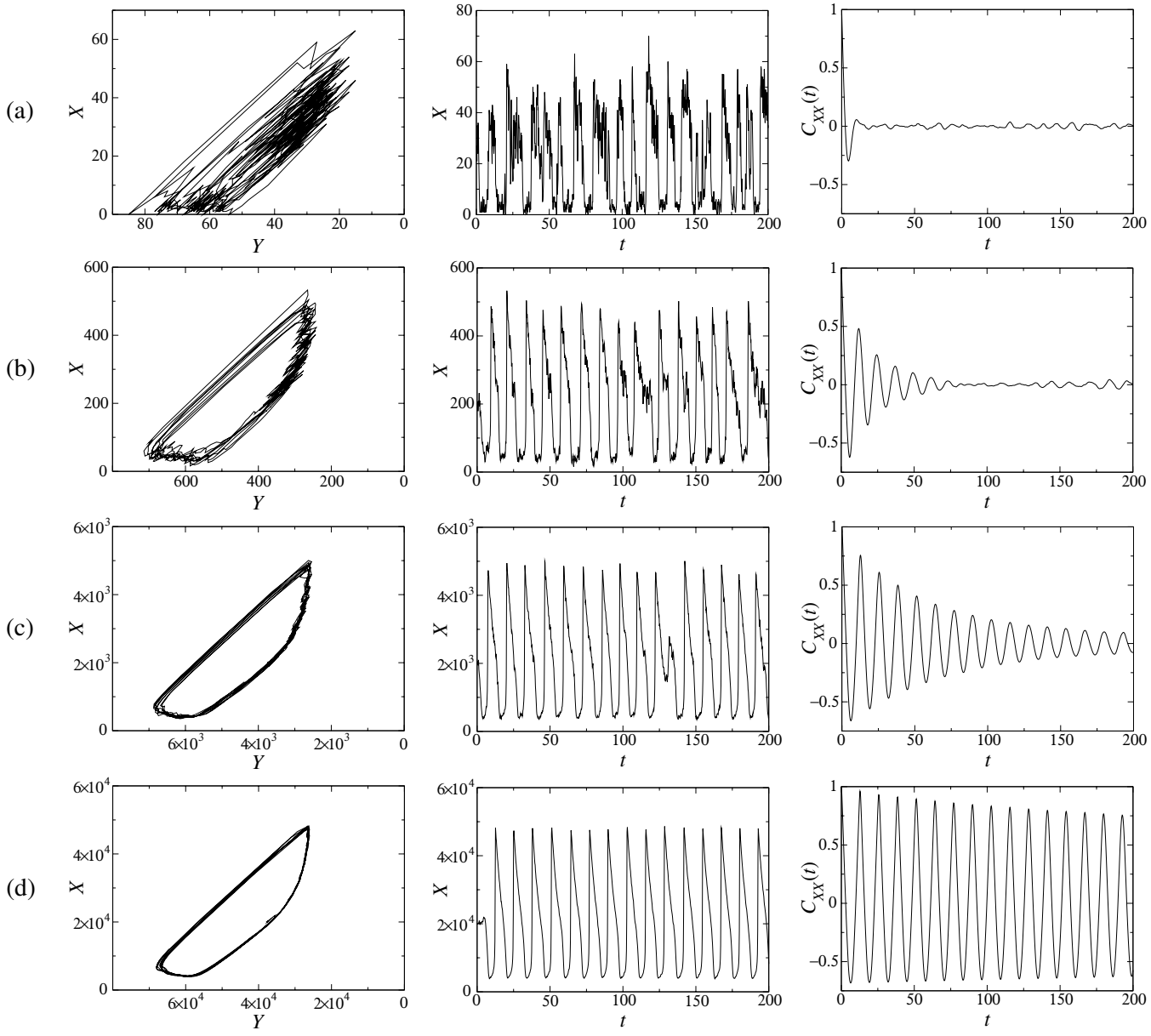


FIG. 1: Simulation by the Gillespie algorithm of the oscillatory regime for the reversible Brusselator (1)-(3). The values of the concentrations are [B] = 7, [A] = [C] = 1, and the reaction constants $k_{+1} = 0.5$, $k_{+2} = k_{+3} = 1$, $k_{-1} = k_{-2} = k_{-3} = 0.25$. From the top to the bottom, the extensivity parameter takes the values: (a) $\Omega = 10$, (b) $\Omega = 100$, (c) $\Omega = 1000$, and (d) $\Omega = 10000$. The first column depicts the phase portrait in the plane of the numbers $X$ and $Y$ of molecules. The second column shows the number $X$ as a function of time. The third one depicts the autocorrelation function (18) of the number $X$, which is normalized to unity.

This phenomenon is illustrated in Fig. 1 for the reversible Brusselator (1)-(3). We observe in the first column

of Fig. 1 the emergence of the closed trajectory in the phase space $(X, Y)$ as the size of the system increases to the macroscopic limit $\Omega \to \infty$. The lower the extensivity parameter, the larger the fluctuations around the mean values of the numbers $X$ and $Y$. In the second column, we see the time dependence of the number $X(t)$. At low values of the extensivity parameter $\Omega$, the number $X(t)$ is so irregular in time that their period is no longer well defined. For increasing values of $\Omega$, the time dependence becomes more and more regular and periodic oscillations progressively emerge. The third column depicts the time autocorrelation function (18) where we can compare the value of the period $T = 2\pi/\omega$ with the correlation time $\gamma^{-1}$. For $\Omega = 10$, the correlation time is of the same order of magnitude as the period, which explains that the signal is too noisy to feature the regularity of a chemical clock. However, the correlation time becomes longer than the period for larger values of $\Omega$. Since the extensivity parameter is proportional to the total number of molecules involved in the reaction, Fig. 1 shows that a nanosystem with a few hundred molecules might be large enough for oscillations to emerge [43].

In the macroscopic limit, the correlation time tends to infinity as the effect of the fluctuations becomes negligible and the deterministic time evolution ruled by the ordinary differential equations (4)-(5) is recovered.

## III. FLUCTUATION THEOREM FOR DISSIPATION

As proposed by Lebowitz and Spohn [5], the breaking of detailed balance due to the nonequilibrium conditions can be evaluated by considering the fluctuating quantity:

$$Z(t) \equiv \ln \frac{W_{\rho_1}(X_0, Y_0|X_1, Y_1)\, W_{\rho_2}(X_1, Y_1|X_2, Y_2)\, \cdots\, W_{\rho_n}(X_{n-1}, Y_{n-1}|X_n, Y_n)}{W_{-\rho_1}(X_1, Y_1|X_0, Y_0)\, W_{-\rho_2}(X_2, Y_2|X_1, Y_1)\, \cdots\, W_{-\rho_n}(X_n, Y_n|X_{n-1}, Y_{n-1})} \tag{19}$$

defined over the random path (17) during some time interval $t$ such that $t_n < t < t_{n+1}$. This so-called action functional increases on average at a rate given by the thermodynamic entropy production and is thus proportional to the amount of dissipation undergone by the system along the random path (17).

The generating function of the fluctuating quantity (19) is defined by

$$q(\eta) \equiv \lim_{t\to\infty} -\frac{1}{t} \ln\langle \mathrm{e}^{-\eta Z(t)}\rangle_{\mathrm{st}} \tag{20}$$

where $\langle\cdot\rangle_{\mathrm{st}}$ denotes the statistical average with respect to the stationary probability distribution. All the statistical moments of the quantity (19) can be obtained by differentiating its generating function (20) at $\eta = 0$. In the steady state, the thermodynamic entropy production is given in terms of the generating according to

$$\frac{d_{\mathrm{i}}S}{dt}\Big|_{\mathrm{st}} = \frac{dq}{d\eta}(0) = \lim_{t\to\infty} \frac{1}{t}\langle Z(t)\rangle_{\mathrm{st}} \geq 0 \tag{21}$$

Now, the generating function (20) obeys the fluctuation theorem

$$q(\eta) = q(1-\eta) \tag{22}$$

as a consequence of the microreversibility [5, 12]. The symmetry (22) can be tested by numerically computing the generating function as an eigenvalue of a differential equation for the conditional expectation value $\langle \mathrm{e}^{-\eta Z(t)}\rangle_{(X,Y)}$ given that the system is initially in the state $(X, Y)$, as explained in Refs. [5, 12]. This differential equation is of the same kind as the master equation and is thus expressed in terms of the transition rates (11)-(16) albeit it also depends on the parameter $\eta$.

The generating function (20) vanishes identically at equilibrium [5, 12]. In the vicinity of equilibrium, the generating function is expected to have the parabolic shape:

$$q(\eta) \simeq \frac{d_{\mathrm{i}}S}{dt}\Big|_{\mathrm{st}} \eta\,(1-\eta) \tag{23}$$

according to Eqs. (21) and (22).

The generating function of the quantity (19) is depicted in Figs. 2 and 3 for two values of the extensivity parameter ($\Omega = 5$ and 15). The bifurcation parameter is taken as the concentration [B]. The other reaction constants and concentrations are fixed at the values $k_{+1} = 0.5$, $k_{+2} = k_{+3} = 1$, $k_{-1} = k_{-2} = k_{-3} = 0.25$, and [A] = [C] = 1. For these parameter values, the equilibrium state is found at $[\mathrm{B}]_{\mathrm{eq}} = 0.0625$, the steady state is a stable node for $0 < [\mathrm{B}] < 4.03024$ and is a stable focus for $4.03024 < [\mathrm{B}] < 6.36667$. The Hopf bifurcation happens at the critical concentration $[\mathrm{B}]_{\mathrm{Hopf}} = 6.36667$. Below this critical value, the steady state of the macroscopic kinetic equations (4)-(5) is an attractor. Above criticality for $6.36667 < [\mathrm{B}]$, the attractor is the limit cycle of Fig. 1.

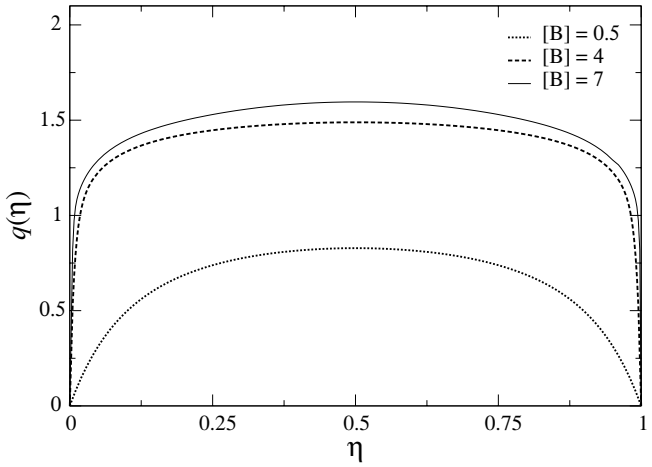


FIG. 2: The generating function (20) numerically obtained for the Brusselator as the eigenvalue by the method of Refs. [5, 12]. The extensivity parameter takes the value $\Omega = 5$ while the control parameter takes the values $[B] = 0.5, 4, 7$. The other parameters are fixed as explained in the text.

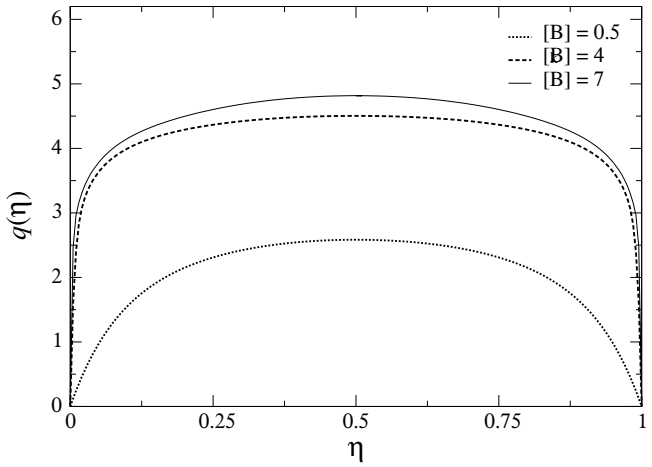


FIG. 3: The generating function (20) numerically obtained for the Brusselator as the eigenvalue by the method of Refs. [5, 12]. The extensivity parameter takes the value $\Omega = 15$ while the control parameter takes the values $[B] = 0.5, 4, 7$. The other parameters are fixed as explained in the text.

In Figs. 2 and 3, the values of the concentration [B] are chosen in order to be relatively close to equilibrium (at [B] = 0.5), near the bifurcation point from the stable node to the stable focus (at [B] = 4), and above the Hopf bifurcation point (at [B] = 7) where the oscillations are well developed. We observe that the symmetry of the fluctuation theorem (22) is perfectly satisfied, showing that successive bifurcations and ultimately the emergence of a limit cycle do not break down the symmetry predicted by the fluctuation theorem. We also see in Figs. 2 and 3 that the far-from-equilibrium driving has no clear effect on the generating function, except for a steep increase of the slope (21) at the origin $\eta = 0$ and strong deviations from the parabola (23) expected in the vicinity of equilibrium. Comparing Figs. 2 and 3, we see that the generating function increases with the extensivity parameter $\Omega$, which can be explained by noting that the thermodynamic entropy production giving the slope at the origin by Eq. (21) is proportional to $\Omega$.

## IV. FLUCTUATION THEOREM FOR CURRENTS

In this section, we consider the fluctuation theorem for currents [13, 15]. In the reversible Brusselator (1)-(3), there is one independent De Donder affinity and one associated macroscopic current for the overall reaction $B \to C$. The De Donder affinity can be defined using the graph theory developed by Hill, Schnakenberg, and others [36, 44, 45].

A graph is associated with the Markov stochastic process of transition rates (11)-(16). The vertices of this graph are all the pairs of non-negative integer numbers of molecules $(X, Y)$. The edges of the graph consist in all the possible transitions between the vertices. Now, cycles can be identified on this graph, such as the cycle from $(X, Y)$ to $(X-1, Y+1)$ by the reaction $+2$ and back to $(X, Y)$ by the reaction $+3$. Since the reversed reactions are also possible due to the fluctuations, the reversed cycle also exists. It turns out that the De Donder affinity can be defined in terms of the ratio of the products of transition rates along the cycle to the one along the reversed cycle as [36]

$$A = \ln \frac{W_{+2}(X,Y|X-1,Y+1)W_{+3}(X-1,Y+1|X,Y)}{W_{-2}(X-1,Y+1|X,Y)W_{-3}(X,Y|X-1,Y+1)} = \ln \frac{k_{+3}k_{+2}\,[\mathrm{B}]}{k_{-3}k_{-2}\,[\mathrm{C}]} \tag{24}$$

The fluctuating quantities of interest are the cumulated currents or fluxes

$$G_\alpha(t) \equiv \int_0^t dt' j_\alpha(t') \tag{25}$$

defined as the time integral of the instantaneous current $j_\alpha(t)$ and corresponding to the signed number of reactive events $\alpha = 2, 3$ occurring over the time interval $t$.

By the method described in Refs. [13, 15], we can derive the fluctuation theorem for the currents, which relates the ratio of the probabilities for opposite signed numbers of reactive events to the exponential of the De Donder affinity multiplied by the random value of the given signed number:

$$\frac{P_{\mathrm{st}}\left[\int_0^t dt' j_\alpha(t') = \xi\, t\right]}{P_{\mathrm{st}}\left[\int_0^t dt' j_\alpha(t') = -\xi\, t\right]} \simeq \exp A\,\xi\, t \qquad \text{for} \quad t \to \infty \tag{26}$$

with the affinity (24). From an operational point of view, such a fluctuation relation could be observed by measuring the number of molecules B (resp. C) which are consumed (resp. produced).

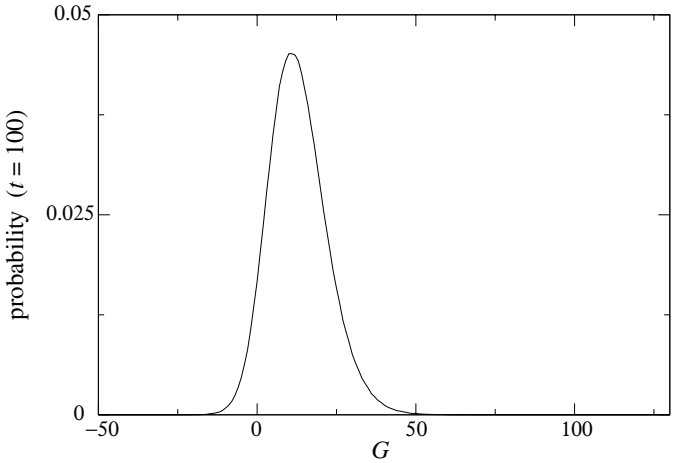


FIG. 4: Probability distribution function for the cumulated current $G$ over a time interval $t = 100$. The concentration [B] is fixed so that the affinity (24) takes the value $A = \ln 1.5$. The other parameters take the values $k_{+1} = 0.5$, $k_{+2} = k_{+3} = 1$, $k_{-1} = k_{-2} = k_{-3} = 0.25$, [A] = [C] = 1, and $\Omega = 1$.

In order to verify the fluctuation theorem (26), we have numerically computed the probability distribution function of the cumulated current $G_t$. This latter is depicted in Fig. 4 for an affinity equal to $A = \ln 1.5$, which is not too far from to equilibrium. This probability distribution function is obtained by direct statistical method. We see in Fig. 4 that the nonlinearities of the model give rise, even in this near-equilibrium regime, to a slightly asymmetric probability distribution function. Clearly, the fluctuations have thus a non-Gaussian character so that the symmetry (26) is not a trivial result even in this near-equilibrium regime.

Indeed, the symmetry of the fluctuation theorem is satisfied as can be seen in Fig. 5, which depicts the generating function of the current defined by

$$\mathrm{e}^{-t\,Q(\lambda)} = \sum_{l=-\infty}^{+\infty} P_{\mathrm{st}}(G_t = l)\,\mathrm{e}^{-\lambda\, l} \tag{27}$$

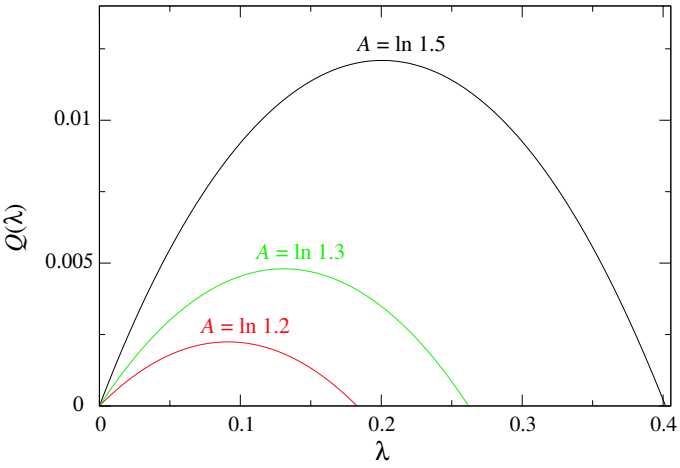


FIG. 5: Probability distribution functions for the cumulated current $G$ over the time interval $t = 100$. The affinity takes the values $A = \ln 1.2$, $\ln 1.3$, and $\ln 1.5$. They obey the symmetry (28). The parameters take the same values as in Fig. 4.

The generating function is shown in Fig. 5 for different values of the affinity (24). In all the cases, the relation

$$Q(\lambda) = Q(A - \lambda) \tag{28}$$

which is equivalent to the symmetry (26) is observed, as announced.

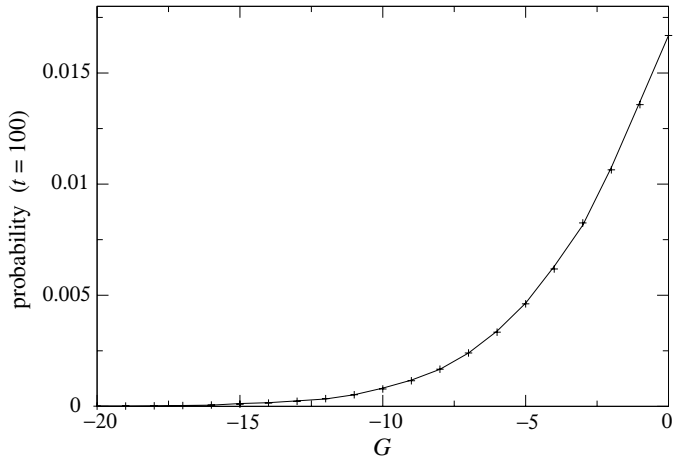


FIG. 6: Probabilities of the negative events (solid line) compared with the predictions (crosses) of the fluctuation relation (29). $G$ is the cumulated current and the affinity takes the value $A = \ln 1.5$. The parameters take the same values as in Fig. 4.

The relation (26) can also be directly verified by comparing the probabilities of the negative events with the prediction the fluctuation theorem according to

$$P_{\rm st}(G_t = -l) \simeq P_{\rm st}(G_t = l)\, {\rm e}^{-A\, l} \tag{29}$$

This relation is very well satisfied as observed in Fig. 6.

We notice that the reaction 1 does not drive the system out of equilibrium as can be seen in the expression (24) of the affinity. Indeed, this reaction cannot sustain any net current otherwise the system would either explode or collapse to a steady state with zero concentration. Nevertheless, the reaction 1 is *sine qua non* to generate a limit cycle and oscillatory behavior: if it was not present, the evolution equation (4)-(5) would conserve the total concentration of molecules $n \equiv x + y$ so that the system would reduce to a one-variable dynamical system. In this case, oscillatory behavior would be impossible since it is well known that oscillations are not possible in unidimensional dynamical systems. This case where the total number of molecules is conserved will be studied in the following section.

## V. THE TRUNCATED MODEL

We saw in the preceding section that the reaction 1 is required to generate the oscillations. We may thus wonder what happens if we consider the Brusselator model without the reaction 1:

$$\mathrm{B} + \mathrm{X} \underset{k_{-2}}{\overset{k_{+2}}{\rightleftharpoons}} \mathrm{Y} + \mathrm{C} \tag{30}$$

$$2\mathrm{X} + \mathrm{Y} \underset{k_{-3}}{\overset{k_{+3}}{\rightleftharpoons}} 3\mathrm{X} \tag{31}$$

In this case, the total number of molecules $N = X + Y$ is a conserved quantity. Our purpose is here to show that, even in this reaction network with a conserved total number of molecules, it is still possible to derive a fluctuation theorem for the current. The construction is essentially the same, with the difference that the state space is here finite and bounded by the states $(X = 0, Y = N)$ and $(X = N, Y = 0)$. However, the boundaries play no role because every path arriving at a boundary in one direction will have to leave in the opposite direction so that the symmetry (26) of the fluctuation theorem is still satisfied with the same affinity (24).

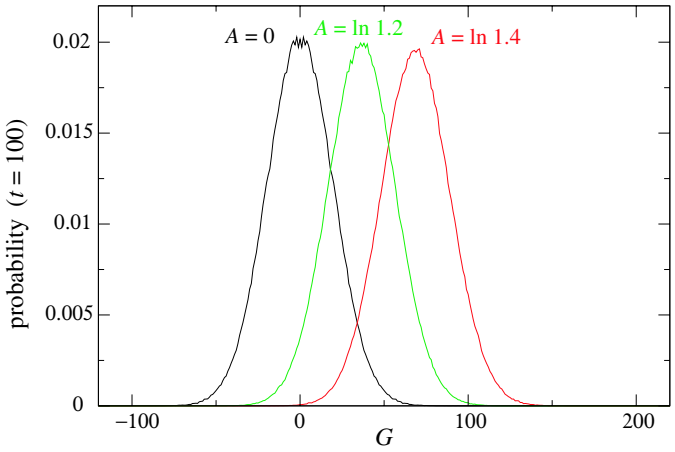


FIG. 7: Probability distribution functions for the cumulated current $G$ over the time interval $t = 100$ in the truncated model (30)-(31). The affinity takes the values $A = 0$, $\ln 1.2$, $\ln 1.4$ for left to right. The concentration [B] is fixed accordingly. The other parameters are $k_{+2} = k_{+3} = 1$, $k_{-2} = k_{-3} = 0.25$, [C] = 1, and $\Omega = 1$.

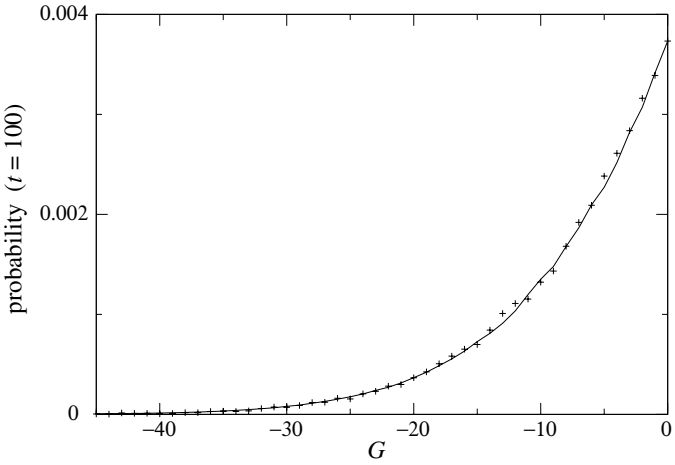


FIG. 8: Probabilities of the negative events (solid line) compared with the predictions (crosses) of the fluctuation relation (29) in the truncated model (30)-(31). $G$ is the cumulated current over the time interval $t = 100$ and the affinity is given by $A = \ln 1.2$. The other parameters take the same values as in Fig. 7.

The probability distribution functions of the current can here also be obtained by direct statistical method and they are depicted in Fig. 7 for different values of the affinity and for $N = 6$. The fluctuation theorem for the current is directly checked in Fig. 8, where we used the fluctuation relation (29) to predict the probability of negative events from the positive ones. The agreement is very good, even for this finite value of the time interval $t$. Accordingly, the fluctuation theorem may also hold in the case the stochastic process has a conserved quantity.

## VI. CONCLUSIONS

In the present paper, we have shown that both the fluctuation theorem for dissipation [5, 12] and the one for the currents [13, 15] hold far from equilibrium in mesoscopic chemical clocks. The condition for the validity of the fluctuation theorems is that the reversed reactions are included in the reaction network. Indeed, the fluctuation theorems characterize the ratio of the probabilities of forward and reversed fluctuations. The farther away from equilibrium, the lower the probability of reversed fluctuations. The fact is that the reversed fluctuations are suppressed by a factor exponentially depending on the magnitude of the De Donder affinities [17]. Accordingly, the reversed probabilities will soon become negligible as the system is driven away from equilibrium. In the limit, the probability of reversed fluctuations may be supposed to vanish, in which case the reactions are fully irreversible with an infinite entropy production.

Therefore, the fluctuation theorems allow us to evaluate the importance of the reversed with respect to the forward fluctuations and to characterize the distance from equilibrium at the level of these fluctuations. These relationships combine the macroscopic concepts of nonequilibrium thermodynamics such as entropy production and the De Donder affinities with the probability distributions of the nonequilibrium fluctuations. In this regard, the fluctuation theorems provide us with the foundations of nonequilibrium statistical thermodynamics.

**Acknowledgments.** The authors thank Professor G. Nicolis for support and encouragement in this research. D. Andrieux is grateful to the F.R.S.-FNRS Belgium for financial support. This research is financially supported by the Belgian Federal Government (IAP project "NOSY"), the "Communauté française de Belgique" (contract "Actions de Recherche Concertées" No. 04/09-312) and the F.R.S.-FNRS Belgium (contract F. R. F. C. No. 2.4577.04).

[1] D. J. Evans, E. G. D. Cohen, and G. P. Morriss, Phys. Rev. Lett. **71**, 2401 (1993).
[2] D. J. Evans and D. J. Searles, Phys. Rev. E **50**, 1645 (1994).
[3] G. Gallavotti and E. G. D. Cohen, Phys. Rev. Lett. **74**, 2694 (1995).
[4] J. Kurchan, J. Phys. A: Math. Gen. **31**, 3719 (1998).
[5] J. L. Lebowitz and H. Spohn, J. Stat. Phys. **95**, 333 (1999).
[6] C. Maes, J. Stat. Phys. **95**, 367 (1999).
[7] G. E. Crooks, Phys. Rev. E **60**, 2721 (1999).
[8] R. van Zon, S. Ciliberto, and E. G. D. Cohen, Phys. Rev. Lett. **92**, 130601 (2004).
[9] U. Seifert, J. Phys. A: Math. Gen. **37**, L517 (2004).
[10] U. Seifert, Phys. Rev. Lett. **95**, 040602 (2005).
[11] S. Rahav and C. Jarzynski, J. Stat. Mech.: Th. Exp. P09012 (2007).
[12] P. Gaspard, J. Chem. Phys. **120**, 8898 (2004).
[13] D. Andrieux and P. Gaspard, J. Chem. Phys. **121**, 6167 (2004); Erratum **125**, 219902 (2006).
[14] D. Andrieux and P. Gaspard, Phys. Rev. E **74**,011906 (2006).
[15] D. Andrieux and P. Gaspard, J. Stat. Phys. **127**, 107 (2007).
[16] D. Andrieux and P. Gaspard, J. Stat. Mech.: Th. Exp. P02006 (2007).
[17] T. De Donder and P. Van Rysselberghe, *Thermodynamic Theory of Affinity* (Stanford University Press, Menlo Park CA, 1936).
[18] I. Prigogine, *Introduction to Thermodynamics of Irreversible Processes* (Wiley, New York, 1967).
[19] G. Nicolis and I. Prigogine, *Self-Organization in Nonequilibrium Systems* (Wiley, New York, 1977).
[20] D. Kondepudi and I. Prigogine, *Modern Thermodynamics: From Heat Engines to Dissipative Structures* (Wiley, Chichester, 1998).
[21] S. K. Scott, *Oscillations, Waves, and Chaos in Chemical Kinetics* (Oxford University Press, Oxford, 1994).
[22] A. M. Zhabotinsky, Biophysika **9**, 306 (1964).
[23] R. J. Field, E. Körös, and R. M. Noyes, J. Am. Chem. Soc. **94**, 8649 (1972).
[24] M. Alamgir, M. Orban, P. De Kepper, and I. R. Epstein, J. Am. Chem. Soc. **105**, 2641 (1983).
[25] M. Orban, C. Dateo, P. De Kepper, and I. R. Epstein, J. Am. Chem. Soc. **104**, 5911 (1982).
[26] A. Goldbeter, *Biochemical Oscillations and Cellular Rhythms* (Cambridge University Press, Cambridge UK, 1996).
[27] D. Gonze, J. Halloy and P. Gaspard, J. Chem. Phys. **116**, 10997 (2002).

[28] R. Imbihl, Prog. Surf. Sci. **44**, 185 (1993).
[29] R. Imbihl and G. Ertl, Chem. Rev. **95**, 697 (1995).
[30] N. Ernst, G. Bozdech, V. Gorodetskii, H.-J. Kreuzer, R. L. C. Wang, and J. H. Block, Surf. Sci. **318**, L1211 (1994).
[31] C. Voss and N. Kruse, Appl. Surf. Sci. **94/95**, 186 (1996).
[32] T. Visart de Bocarmé and N. Kruse, Chaos **12**, 118 (2002).
[33] G. Nicolis, J. Stat. Phys. **6**, 195 (1972).
[34] M. Malek-Mansour and G. Nicolis, J. Stat. Phys. **13**, 197 (1975).
[35] Luo Jiu-li, C. Van den Broeck, and G. Nicolis, Z. Phys. B - Condensed Matter **56**, 165 (1984).
[36] J. Schnakenberg, Rev. Mod. Phys. **48**, 571 (1976).
[37] I. Prigogine and R. Lefever, J. Chem. Phys. **48**, 1695 (1968).
[38] R. Lefever, G. Nicolis, and P. Borckmans, J. Chem. Soc., Faraday Trans. 1 **84**, 1013 (1988).
[39] F. Baras, J. E. Pearson, and M. Malek Mansour, J. Chem. Phys. **93**, 5747 (1990).
[40] G. Nicolis, *Introduction to Nonlinear Science* (Cambridge University Press, Cambridge UK, 1995).
[41] D. T. Gillespie, J. Comput. Phys. **22**, 403 (1976).
[42] D. T. Gillespie, J. Phys. Chem. **81**, 2340 (1977).
[43] P. Gaspard, J. Chem. Phys. **117**, 8905 (2002).
[44] T. L. Hill, *Free Energy Transduction and Biochemical Cycle Kinetics* (Dover, New York, 2005).
[45] D.-Q. Jiang, M. Qian, and M.-P. Qian, *Mathematical Theory of Nonequilibrium Steady States* (Springer, Berlin, 2004).